

## Soft-mode behavior of electromagnons in multiferroic manganite

A. M. Shuvaev,<sup>1</sup> J. Hemberger,<sup>2</sup> D. Niermann,<sup>2</sup> F. Schrettle,<sup>3</sup> A. Loidl,<sup>3</sup> V. Yu. Ivanov,<sup>4</sup> V. D. Travkin,<sup>4</sup> A. A. Mukhin,<sup>4</sup> and A. Pimenov<sup>1</sup>

<sup>1</sup>*Experimentelle Physik IV, Universität Würzburg, 97074 Würzburg, Germany*

<sup>2</sup>*II. Physikalisches Institut, Universität zu Köln, 50937 Köln, Germany*

<sup>3</sup>*Experimentalphysik V, EKM, Universität Augsburg, 86135 Augsburg, Germany*

<sup>4</sup>*General Physics Institute, Russian Academy of Sciences, 119991 Moscow, Russia*

(Received 14 July 2010; revised manuscript received 6 September 2010; published 12 November 2010)

The behavior of the low-frequency electromagnon in multiferroic DyMnO<sub>3</sub> has been investigated in external magnetic fields and in a magnetically ordered state. Significant softening of the electromagnon frequency is observed for external magnetic fields parallel to the *a* axis (*B*∥*a*), revealing a number of similarities to a classical soft-mode behavior known for ferroelectric phase transitions. The softening of the electromagnon yields an increase in the static dielectric permittivity which follows a similar dependence as predicted by the Lyddane-Sachs-Teller relation. Within the geometry *B*∥*b* the increase in the electromagnon intensity does not correspond to the softening of the eigenfrequency. In this case the increase in the static dielectric permittivity seems to be governed by the motion of the domain walls.

DOI: [10.1103/PhysRevB.82.174417](https://doi.org/10.1103/PhysRevB.82.174417)

PACS number(s): 75.85.+t, 75.47.Lx, 78.30.-j, 75.30.Ds

### I. INTRODUCTION

Soft modes have long been studied in connection with structural phase transitions in crystalline solids.<sup>1-3</sup> Close to such phase transition the frequency of the normally lowest lattice vibration strongly decreases<sup>4</sup> (softens) as a result of a “flattening” of an effective potential. Therefore, soft modes reflect an instability of the crystal lattice<sup>5</sup> and are often accompanied by a substantial nonlinearity of the system. Especially in ferroelectric crystals the softening of a lattice vibration is followed by a divergence of the static dielectric permittivity. In a simple case a lattice vibration can be written in the Lorentz form

$$\varepsilon(\omega) = \varepsilon_\infty + \frac{\Delta\varepsilon \cdot \omega_r^2}{\omega_r^2 - \omega^2 - i\omega\gamma} = \varepsilon_\infty \frac{\omega_{LO}^2 - \omega^2 - i\omega\gamma}{\omega_r^2 - \omega^2 - i\omega\gamma}. \quad (1)$$

Here  $\omega_r$  is the resonance frequency,  $\omega_{LO}$  is the frequency of the longitudinal phonon,  $\gamma$  is the damping,  $\varepsilon_\infty$  is the high-frequency permittivity, and  $\Delta\varepsilon$  is the dielectric contribution of the mode to the static dielectric permittivity. From this equation the well-known Lyddane-Sachs-Teller (LST) relation immediately follows<sup>3</sup>

$$\varepsilon(0)/\varepsilon_\infty = (\varepsilon_\infty + \Delta\varepsilon)/\varepsilon_\infty = [\omega_{LO}/\omega_r]^2. \quad (2)$$

Close to structural phase transition in ferroelectrics  $\omega_r$  softens and  $\omega_{LO}$  basically remains constant,<sup>1</sup> which leads to the mentioned divergence of the static dielectric permittivity.

Physically similar conclusion can be drawn taking into account that the spectral weight of a single excitation is often conserved. In spectroscopy this is generally termed as a sum rule and can be derived from first principles.<sup>6</sup> The spectral weight is proportional to the electron density and can be written as

$$S \sim \int_0^\infty \omega \text{Im}[\varepsilon(\omega)] d\omega \sim \Delta\varepsilon \cdot \omega_r^2. \quad (3)$$

Evidently, in order to preserve the constant spectral weight with decreasing resonance frequency, the dielectric contribution must diverge as  $\Delta\varepsilon \sim 1/\omega_r^2$ . The last formula works well for the soft lattice vibrations and represents another form of the LST relation.

Although governed by different mechanisms, qualitatively similar effects can be observed in glassy materials as well. In this case a broad structural relaxation mode, called alpha relaxation,<sup>7</sup> moves toward zero frequency reflecting the freezing of the ionic movement. Contrary to the crystalline solids, in glasses the situation is more complicated and the spectral weight of the structural relaxation is not conserved. However, the divergence of the static dielectric constant close to glass transition has been put into discussion for non-crystalline solids as well.<sup>8</sup>

Another sum rule can be derived in case of dielectric spectroscopy, which of course correlates with the conservation of the spectral weight. This sum-rule states that the static dielectric permittivity can be calculated as a sum of all contributions from absorption processes at finite frequencies.<sup>6</sup> Therefore, in experiment one might try to always correlate the changes in static properties with changes in the absorption spectra at finite frequencies. As a characteristic example, the suppression of an electroactive mode in multiferroic GdMnO<sub>3</sub> and TbMnO<sub>3</sub> has been put forward as a spectroscopic explanation of field-induced changes in the static dielectric constant.<sup>9</sup>

Multiferroics represent an intriguing class of materials in which electric and magnetic orders coexist.<sup>10-12</sup> Most interesting effects occur if both orders are strongly coupled. This leads to such effects like the control of electric polarization by external magnetic field or the control of magnetization by electric field. In addition to static polarization, dynamic properties of multiferroics are very rich and in various com-

pounds show the existence of a series of new excitations. These excitations are electrically active magnetic modes of the cycloidal spin structure and they have been called electromagnons.<sup>13,14</sup> The electromagnons may be suppressed in external magnetic field leading to substantial changes in the dielectric permittivity in a broad frequency range.

DyMnO<sub>3</sub> belongs to the most studied multiferroic manganites with orthorhombic structure. Below the Néel phase transition at  $T=39$  K DyMnO<sub>3</sub> first possesses an incommensurate magnetic order.<sup>15–17</sup> For  $T \leq 19$  K this order turns into a spin cycloid with the manganese spins rotating in the crystallographic  $bc$  plane. As has been proven both theoretically and experimentally, this spin structure leads to the occurrence of the static electric polarization parallel to the  $c$  axis.<sup>16,18,19</sup> Similar to such multiferroics such as GdMnO<sub>3</sub> or TbMnO<sub>3</sub>, DyMnO<sub>3</sub> shows the series of electromagnons at finite frequencies, which basically consists of two modes at 2 meV and 6 meV (15 cm<sup>-1</sup> and 50 cm<sup>-1</sup>), respectively.<sup>13,20,21</sup> Although the physical mechanism of the electromagnons is not fully understood until now, the high-frequency mode seems to correspond to a zone-boundary magnon.<sup>22,23</sup> This magnon acquires electric dipole activity and becomes visible in the optical spectra as a result of the Heisenberg exchange mechanism combined with the cycloidal spin structure. The up-to-date situation with the low-frequency electromagnon is a bit more complicated. According to recent experimental results<sup>24,25</sup> on the closely similar multiferroic TbMnO<sub>3</sub>, the low-frequency electromagnon corresponds to an eigenmode of the cycloidal spin structure<sup>26</sup> which becomes infrared active due to an incommensurate spin modulation of the cycloid. We note that an alternative explanation based on anisotropic effects has been suggested as well.<sup>27,28</sup>

In this work we present the comparison of the electromagnon dynamics in external magnetic fields with the changes in the static dielectric permittivity in the multiferroic DyMnO<sub>3</sub>. Substantial decrease in the electromagnon frequency is observed in the cycloidal magnetic phase. This softening behavior correlates with an increase in the static dielectric permittivity, thus revealing similar dependence as predicted by the Lyddane-Sachs-Teller relation.

## II. EXPERIMENTAL DETAILS

The spectroscopic experiments in the terahertz frequency range ( $3 \text{ cm}^{-1} < \nu < 40 \text{ cm}^{-1}$ ) have been carried out in a Mach-Zehnder interferometer arrangement<sup>29,30</sup> which allows measurements of the amplitude and the phase shift in a geometry with controlled polarization of radiation. Dynamic dielectric properties  $\varepsilon^*(\omega, B) = \varepsilon_1 + i\varepsilon_2$  were calculated from these quantities using the Fresnel optical equations for the complex transmission coefficient. The experiments in external magnetic fields up to 8 T have been performed in a superconducting split-coil magnet with polypropylene windows. A frequency-response analyzer (Novocontrol alpha analyzer) was used for static dielectric measurements. Single crystals of DyMnO<sub>3</sub> have been grown using the floating-zone method with radiation heating. The samples were characterized using x-ray, magnetic, dielectric, and optical measurements.<sup>13,31</sup> The results of these experiments includ-

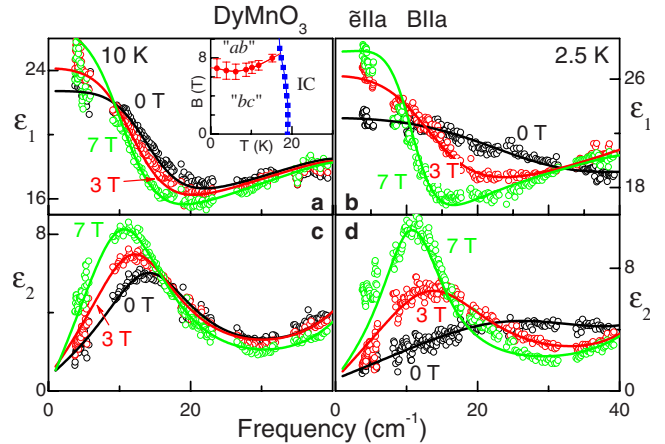


FIG. 1. (Color online) Frequency dependence of the [(a) and (b)] real and [(c) and (d)] imaginary parts of the dielectric permittivity  $\varepsilon^* = \varepsilon_1 + i\varepsilon_2$  of DyMnO<sub>3</sub> along the  $a$  axis for different temperatures and external magnetic fields. For increasing magnetic fields a softening and a growth of intensity of the electromagnon is clearly observed. The inset shows the  $(B, T)$  phase diagram for static magnetic fields along the  $a$  axis (Ref. 16). IC— incommensurate magnetic state, “ $ab$ ” and “ $bc$ ” denote the  $ab$ -plane and the  $bc$ -plane oriented cycloids, respectively. Error bars for the  $bc$ - $ab$  transition reflect the hysteresis and history dependence in different experiments.  $\vec{e}$  indicates the ac electric field of the electromagnetic wave.

ing the magnetic phase diagrams are closely similar to the published results.<sup>16</sup>

## III. RESULTS AND DISCUSSION

### A. $B \parallel a$

Figure 1 shows the spectra of the low-frequency electromagnon in DyMnO<sub>3</sub>, which have been obtained in the magnetically ordered state with the spin cycloid oriented in the crystallographic  $bc$  plane. This phase is indicated as “ $bc$ ” in the phase diagram<sup>16</sup> shown in the inset of Fig. 1. Application of an external magnetic field parallel to the crystallographic  $a$  axis leads to a rotation of the  $bc$  cycloid around the  $b$  axis from the  $bc$  plane to the  $ab$  plane.<sup>32</sup> Because both static and terahertz properties in DyMnO<sub>3</sub> depend on the details of the spin structure, the changes in the electromagnon spectra can be expected in external magnetic fields as well. Indeed, the spectra in Fig. 1 clearly demonstrate that in external magnetic fields  $B \parallel a$  the initial electromagnon mode (black symbols and lines, 0 T) shifts to lower frequencies and gains intensity. This effect is especially strong for the data at  $T = 2.5$  K (right panels in Fig. 1). However, in this temperature range the ordering of the Dy moments may play an important role. Therefore, in the qualitative analysis given below, we concentrate on the results at  $T = 10$  K, i.e., in the state without Dy order (left panels). The shifting of the electromagnon mode to lower frequencies is accompanied by a substantial increase in the amplitude. This behavior reveals already at this point a close similarity to classical soft modes. In order to investigate this similarity in more details, we have carried out the qualitative analysis of the electromagnon using the

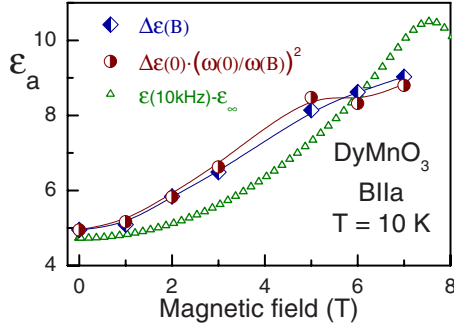


FIG. 2. (Color online) Comparison of the static and dynamic properties of  $\text{DyMnO}_3$  along the  $a$  axis. Diamonds represent the measured dielectric contribution of the electromagnon. Circles—dielectric contribution of the electromagnon as predicted by the LST relation. Triangles—static dielectric permittivity with a high-frequency value  $\varepsilon_\infty=25$  subtracted.

sum of two Lorentz oscillators as a model for the dielectric permittivity. The second oscillator is necessary to take into account the influence of the second electromagnon<sup>20</sup> around  $50 \text{ cm}^{-1}$  and of the low-frequency tail of the phonon contribution. For simplicity, we assumed the field independence of the parameters of the high-frequency electromagnon. Approximate field independence of our spectra above  $\sim 30 \text{ cm}^{-1}$  supports this assumption.

Figure 2 shows the magnetic field dependence of the dielectric contribution of the electromagnon (diamonds) as obtained from the fits of the spectra. As already expected from the qualitative analysis of the spectra in Fig. 1, the dielectric contribution  $\Delta\varepsilon$  of the low-frequency electromagnon shows an increase by more than a factor of 2 as approaching the phase transition to the  $ab$ -oriented spiral around 7 T. These data can now be compared to the magnetic field dependence of the static dielectric permittivity which is shown by the green triangles on the same scale. Here we subtracted the field-independent value of the high-frequency permittivity for clarity. Comparing these two data sets it becomes clear that the magnetic field dependencies of high- and low-frequency data are closely similar. According to the sum rule for the static dielectric permittivity<sup>6</sup>

$$\varepsilon_1(0) - 1 = \frac{2}{\pi} \int_0^\infty \frac{\varepsilon_2(\omega)}{\omega} d\omega = \sum_i \Delta\varepsilon^i, \quad (4)$$

the static permittivity is the sum of all contributions  $\Delta\varepsilon^i$  of all high-frequency processes. The last equality in Eq. (4) is written assuming a Lorentzian shape, Eq. (1), of all excitations. Therefore, at this point we may conclude that the changes in  $\varepsilon(10 \text{ KHz})$  are governed by the electromagnon excitation at  $10 \text{ cm}^{-1}$  and no other excitations substantially contribute to the magnetic field dependence of the static permittivity.

As already mentioned in the discussion of Fig. 1, the changes in the static dielectric constant and the dielectric contribution of the low-frequency electromagnon closely correlate with the decrease in the resonance frequency. This is demonstrated in Fig. 2 by plotting  $\Delta\varepsilon[\omega(0)/\omega(B)]^2$  (circles). This plot corresponds directly to the Lyddane-

Sachs-Teller relation, Eq. (2), i.e., the increase in the static permittivity is inversely proportional to the square of the resonance frequency of the low-energy electromagnon. Because in agreement to Eq. (3) the dielectric contribution is proportional to  $1/\omega_r^2$  as well, the observed LST similar behavior reflects the conservation of the spectral weight of the electromagnon in external magnetic fields along the  $a$  axis.

We note that a correspondence of lattice soft modes and electromagnons is not straightforward. The latter are defined in the ordered state and reveal critical behavior approaching a phase transition as function of magnetic field. The LST-derived equation for  $\text{DyMnO}_3$  relates the dielectric constant at zero magnetic fields to that in finite fields while it relates transverse and longitudinal modes in dielectrics. The softening of the electromagnon in external fields can be qualitatively understood taking into account the switching of the orientation of the spin cycloid. Similar to many other structural transitions the effective stiffness of the cycloid probably tends to zero on the phase border between the  $bc$  and  $ab$  cycloids, leading to a softening of the electromagnon. The unresolved question is: why the spectral weight of the electromagnon is conserved during the softening of the eigenfrequency? In case of classical softening of the lattice vibration one normally argues that the spectral weight of the soft mode is directly connected to the total number of electrons in the material. In agreement with the charge conservation a constant spectral weight may be expected for soft phonons. In case of a magnetic cycloid the electromagnon gains the spectral weight as a result of a complex interplay of various mechanisms. Therefore, we cannot use the conservation of the magnetic moment as an argument, and the observed conservation of the spectral weight remains an actual problem.

### B. $B\parallel b$

We turn now to the experimental geometry in which the transition from the  $bc$  to the  $ab$  cycloid is achieved by external magnetic fields along the  $b$  axis. Although here some hints to a soft-mode behavior could be detected as well, the results turned out to be more complicated to interpret. Contrary to the results of the previous section, here we could not observe the similarity between the behavior of the electromagnon and the LST relation. Therefore, the data for this geometry will be presented with less details and for one characteristic temperature only.

Figure 3 shows the terahertz spectra of the electromagnon in the geometry  $B\parallel b$ . We note at this point that previously the terahertz spectra for this field geometry have been obtained in Ref. 20. Similar to the results in the previous section (Fig. 1), the spectra in the geometry  $B\parallel b$  reveal an increase in the electromagnon intensity in external magnetic fields. However, already the comparison of the spectra at 6 and 2 T suggests that the increase in the mode intensity is not directly correlated with the decrease in the resonance frequency. Even without exact analysis of the fits one can see that the maxima in  $\varepsilon_2$  for 2 T and 6 T roughly coincide in spite of substantially different intensities. To carry out the qualitative analysis, these spectra have been analyzed using the Lorentz oscillator model. The contribution from the high-

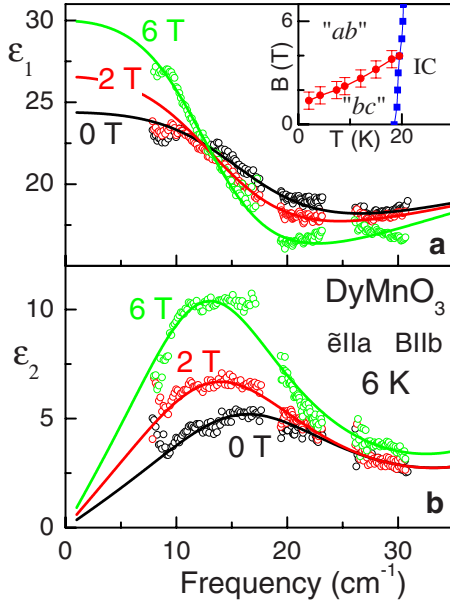


FIG. 3. (Color online) Frequency dependence of the [(a) and (b)] real and [(c) and (d)] imaginary parts of the dielectric permittivity of DyMnO<sub>3</sub> for  $\vec{e}||a$  for different external magnetic fields  $B||b$  and at  $T=6$  K. The inset shows the  $(B, T)$  phase diagram (Ref. 16) for static magnetic fields along the  $b$  axis. Notations are the same as in Fig. 1.

frequency processes has been accounted for using a high-frequency excitation with the field-independent parameters. The results of the quantitative analysis of the spectra within this geometry are shown in Fig. 4.

Figure 4 presents the comparison of the static and dynamic properties of DyMnO<sub>3</sub> for the geometry  $B||b$ . Similar to the results for  $B||a$  the dielectric contribution of the electromagnon (diamonds) increases in external magnetic fields parallel to the  $b$  axis. However, the changes in the static dielectric permittivity in the fields  $B||b$  do not directly correlate with the behavior of the static dielectric permittivity because the latter is dominated by a strong peak at  $B=2$  T. Most probably, to describe this peak in the static

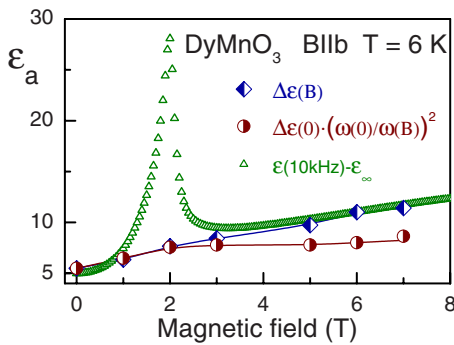


FIG. 4. (Color online) Comparison of the static and dynamic properties of DyMnO<sub>3</sub> for  $\vec{e}||a$  and  $B||b$ . Diamonds represent the measured dielectric contribution of the electromagnon. Circles—dielectric contribution of the electromagnon as predicted by the LST relation. Triangles—static dielectric permittivity with a high-frequency value  $\epsilon_\infty=25$  subtracted.

permittivity an additional process has to be taken into account. In this case we refer to the recent paper<sup>33</sup> by Kagawa *et al.* in which the dielectric contribution of the domain walls in DyMnO<sub>3</sub> has been investigated. It has been shown that the peak in the dielectric constant around  $bc$ -to- $ab$  phase transition is due to a domain-wall relaxation with characteristic frequency situated in the radio wave range. It has been shown that the relaxation rate of the domain-wall motion (Fig. 2 of Ref. 33) correlates well with the peak position of the static dielectric permittivity. Therefore, we may conclude that the peak in the static permittivity close to  $B=2$  T (Fig. 4) comes from the dielectric contribution of the domain walls. Within the notations of Eq. (4) the motion of the domain walls represents one of the contributions to the static permittivity. On the other hand, far from the critical value of 2 T a correlation between the electromagnon contribution  $[\Delta\epsilon(B), \text{diamonds}]$  and static permittivity  $[\epsilon(10 \text{ kHz}, \text{triangles})]$  seem to be restored. Indeed, above approximately 3 T both curves follow the same increasing behavior with a slope of about  $1.5 \text{ T}^{-1}$ . In agreement with the sum rule, this indicates that this increase is solely due to the influence of the electromagnon.

Red circles in Fig. 4 represent the eigenfrequency of the electromagnon in the geometry  $B||b$ . In order to make the same comparison as in previous section, we plot the inverse electromagnon frequency normalized as  $\Delta\epsilon[\omega(0)/\omega(B)]^2$ , where  $\Delta\epsilon$  and  $\omega(0)$  are the values of the eigenfrequency and the dielectric contribution in zero field. As seen qualitatively during the discussion of Fig. 3, the electromagnon frequency remains basically constant in this geometry. This indicates that for these data the LST relation does not hold which partly can be explained by strong influence of the domain-wall motion on the dielectric properties.

#### IV. CONCLUSIONS

The behavior of the electromagnon in DyMnO<sub>3</sub> in external magnetic fields has been investigated and compared to the changes in the static dielectric permittivity. A softening of the electromagnon is observed for external magnetic fields parallel to the  $a$  axis, which is accompanied by an increase in the dielectric strength and of the static permittivity. Our results demonstrate that a soft-modelike behavior with a substantial increase in the static dielectric constant can be observed for electromagnons as well. In this case a magnetolectric mode becomes soft and an external magnetic field serves as a driving parameter for this behavior. The observed similarity reveals further close connection between multiferroics and classical ferroelectrics. For magnetic fields parallel to the  $b$  axis no direct correlation between the electromagnon frequency and the static dielectric permittivity exists. In this case the static properties seem to be governed by a motion of the domain walls.

#### ACKNOWLEDGMENTS

We acknowledge fruitful discussion with P. Lunkenheimer. This work was supported by DFG (Pi 372).

- <sup>1</sup>R. Blinc and B. Žekš, *Soft Modes in Ferroelectrics and Antiferroelectrics* (North-Holland, Amsterdam, 1974).
- <sup>2</sup>W. Cochran, *Adv. Phys.* **9**, 387 (1960).
- <sup>3</sup>J. F. Scott, *Rev. Mod. Phys.* **46**, 83 (1974).
- <sup>4</sup>J. Petzelt, G. V. Kozlov, and A. A. Volkov, *Ferroelectrics* **73**, 101 (1987).
- <sup>5</sup>R. A. Cowley, *Adv. Phys.* **29**, 1 (1980).
- <sup>6</sup>M. Dressel and G. Grüner, *Electrodynamics of Solids: Optical Properties of Electrons in Matter*, 1st ed. (Cambridge University Press, Cambridge, 2002).
- <sup>7</sup>P. Lunkenheimer, U. Schneider, R. Brand, and A. Loidl, *Contemp. Phys.* **41**, 15 (2000).
- <sup>8</sup>N. Menon and S. R. Nagel, *Phys. Rev. Lett.* **74**, 1230 (1995).
- <sup>9</sup>A. Pimenov, A. A. Mukhin, V. Y. Ivanov, V. D. Travkin, A. M. Balbashov, and A. Loidl, *Nat. Phys.* **2**, 97 (2006).
- <sup>10</sup>M. Fiebig, *J. Phys. D: Appl. Phys.* **38**, R123 (2005).
- <sup>11</sup>Y. Tokura, *Science* **312**, 1481 (2006).
- <sup>12</sup>W. Eerenstein, N. D. Mathur, and J. F. Scott, *Nature (London)* **442**, 759 (2006).
- <sup>13</sup>A. Pimenov, A. M. Shuvaev, A. A. Mukhin, and A. Loidl, *J. Phys.: Condens. Matter* **20**, 434209 (2008).
- <sup>14</sup>A. B. Sushkov, M. Mostovoy, R. V. Aguilar, S.-W. Cheong, and H. D. Drew, *J. Phys.: Condens. Matter* **20**, 434210 (2008).
- <sup>15</sup>T. Kimura, S. Ishihara, H. Shintani, T. Arima, K. T. Takahashi, K. Ishizaka, and Y. Tokura, *Phys. Rev. B* **68**, 060403 (2003).
- <sup>16</sup>T. Kimura, G. Lawes, T. Goto, Y. Tokura, and A. P. Ramirez, *Phys. Rev. B* **71**, 224425 (2005).
- <sup>17</sup>R. Feyerherm, E. Dudzik, N. Aliouane, and D. N. Argyriou, *Phys. Rev. B* **73**, 180401 (2006).
- <sup>18</sup>S.-W. Cheong and M. Mostovoy, *Nature Mater.* **6**, 13 (2007).
- <sup>19</sup>T. Goto, T. Kimura, G. Lawes, A. P. Ramirez, and Y. Tokura, *Phys. Rev. Lett.* **92**, 257201 (2004).
- <sup>20</sup>N. Kida, Y. Ikebe, Y. Takahashi, J. P. He, Y. Kaneko, Y. Yamasaki, R. Shimano, T. Arima, N. Nagaosa, and Y. Tokura, *Phys. Rev. B* **78**, 104414 (2008).
- <sup>21</sup>N. Kida, Y. Takahashi, J. S. Lee, R. Shimano, Y. Yamasaki, Y. Kaneko, S. Miyahara, N. Furukawa, T. Arima, and Y. Tokura, *J. Opt. Soc. Am. B* **26**, A35 (2009).
- <sup>22</sup>R. Valdés Aguilar, M. Mostovoy, A. B. Sushkov, C. L. Zhang, Y. J. Choi, S.-W. Cheong, and H. D. Drew, *Phys. Rev. Lett.* **102**, 047203 (2009).
- <sup>23</sup>J. S. Lee, N. Kida, S. Miyahara, Y. Takahashi, Y. Yamasaki, R. Shimano, N. Furukawa, and Y. Tokura, *Phys. Rev. B* **79**, 180403 (2009).
- <sup>24</sup>A. Pimenov, A. Shuvaev, A. Loidl, F. Schrettle, A. A. Mukhin, V. D. Travkin, V. Y. Ivanov, and A. M. Balbashov, *Phys. Rev. Lett.* **102**, 107203 (2009).
- <sup>25</sup>A. M. Shuvaev, V. D. Travkin, V. Y. Ivanov, A. A. Mukhin, and A. Pimenov, *Phys. Rev. Lett.* **104**, 097202 (2010).
- <sup>26</sup>D. Senff, N. Aliouane, D. N. Argyriou, A. Hiess, L. P. Regnault, P. Link, K. Hradil, Y. Sidis, and M. Braden, *J. Phys.: Condens. Matter* **20**, 434212 (2008).
- <sup>27</sup>M. P. V. Stenberg and R. de Sousa, *Phys. Rev. B* **80**, 094419 (2009).
- <sup>28</sup>M. Mochizuki, N. Furukawa, and N. Nagaosa, *Phys. Rev. Lett.* **104**, 177206 (2010).
- <sup>29</sup>A. A. Volkov, Y. G. Goncharov, G. V. Kozlov, S. P. Lebedev, and A. M. Prokhorov, *Infrared Phys.* **25**, 369 (1985).
- <sup>30</sup>A. Pimenov, S. Tachos, T. Rudolf, A. Loidl, D. Schrupp, M. Sing, R. Claessen, and V. A. M. Brabers, *Phys. Rev. B* **72**, 035131 (2005).
- <sup>31</sup>F. Schrettle, P. Lunkenheimer, J. Hemberger, V. Y. Ivanov, A. A. Mukhin, A. M. Balbashov, and A. Loidl, *Phys. Rev. Lett.* **102**, 207208 (2009).
- <sup>32</sup>R. Feyerherm *et al.*, *Phys. Rev. B* **79**, 134426 (2009).
- <sup>33</sup>F. Kagawa, M. Mochizuki, Y. Onose, H. Murakawa, Y. Kaneko, N. Furukawa, and Y. Tokura, *Phys. Rev. Lett.* **102**, 057604 (2009).